Extended Abstracts of the 2019 International Conference on Solid State Devices and Materials, Nagoya, 2019, pp1009-1010

# Influence of Dopant on Thermoelectric Properties of Si-rich Poly-$Si_{1-x}Sn_x$ Layers Grown on Insulators

Kei Sato[1], Osamu Nakatsuka[1,2] and Masashi Kurosawa[1,3,4*]

[1] Graduate School of Engineering, Nagoya University, Furo-cho, Chikusa-ku, Nagoya 464-8603, Japan
[2] Institute of Materials and Systems for Sustainability, Nagoya University, Furo-cho, Chikusa-ku, Nagoya 464-8603, Japan
[3] Institute for Advanced Research, Nagoya University, Furo-cho, Chikusa-ku, Nagoya 464-8601, Japan
[4] PRESTO, Japan Science and Technology Agency, 4-1-8, Honcho, Kawaguchi, Saitama 332-0012, Japan
*Phone: +81-52-789-3819 E-mail: kurosawa@nagoya-u.jp

**Abstract**

**Thermoelectric properties of boron or phosphorus-doped polycrystalline $Si_{1-x}Sn_x$ ($x<0.1$) layers grown on $SiO_2$ by solid-phase crystallization have been firstly demonstrated. The incorporation of 10 % Sn could reduce the crystallization temperature from 900 to 500 °C regardless of the existence of the dopants. A higher power factor of 0.53 $\mu Wcm^{-1}K^{-2}$ was obtained for boron-doped $Si_{1-x}Sn_x$ layers, which may depend on whether dopant segregation occurs or not.**

## 1. Introduction

Integration of thin-film thermoelectric generators (TEGs), which could convert waste heat into electricity, in an expensive substrate such as Si chip is strongly desired for realizing standalone sensing network system, called internet-of-things (IoT) society, coupled with low-power consumption technologies. Taking distributing a huge number of sensors all over the world into consideration, utilization of the same technology to manufacture next-generation Si integrated circuits is preferable, including the material.

Tin-incorporated Si, which is called Si-rich $Si_{1-x}Sn_x$ in this report, theoretically possesses the lowest thermal conductivity among group-IV binary alloys [1] owing to the mass-difference scattering of phonons. Thermoelectric efficiency is inversely proportional to the thermal conductivity. Hence, the $Si_{1-x}Sn_x$ is one of the attractive materials. We have been investigated the crystal growth of undoped [2,3] or gallium-doped [4] $Si_{1-x}Sn_x$ layers on various substrates; the thermoelectric properties, however, have not been understood. Therefore, in this study, we aim to reveal the thermoelectric properties of p- and n-type Si-rich polycrystalline (poly-) $Si_{1-x}Sn_x$ layers grown on $SiO_2$ by solid-phase crystallization (SPC).

## 2. Experimental procedure

A Si(001) wafer covered with a 1-μm-thick $SiO_2$ layer was used as the substrates. A 300-nm-thick amorphous (a-) Si or a-$Si_{1-x}Sn_x$ layer with a Sn content of 2% was deposited on the substrates at room temperature (RT) using an RF sputtering system in Ar ambient with a pressure of 0.1 Pa. Boron (B) or phosphorus (P) ions at a dose of $1\times10^{15}$ $cm^{-2}$ were doped into the amorphous layers using ion implantation method, where the energy for B (P) was 70 (120) keV. Note that a 15-nm-thick $SiO_2$ layer was used only for P-doped samples. Finally, to induce polycrystallization and dopant activation, these samples were annealed at various temperatures between 500 and 900 °C for 10 min in a dry $N_2$ ambient.

## 3. Results and discussion

To clarify the effect of Sn incorporation on the crystallization temperature of Si, Raman scattering spectroscopy was performed. Figures 1(a) and 1(b) show the Raman spectra of the B-doped Si and $Si_{1-x}Sn_x$ samples, respectively. For the Si layer without Sn [Fig. 1(a)], only one broad peak at around 470 $cm^{-1}$ was observed before and after annealing below 700 °C. With increasing the annealing temperature to 900 °C, additional clear peaks (around 500 and 520 $cm^{-1}$) were observed, suggesting polycrystals with small grains [5]. On the other hand, for the $Si_{1-x}Sn_x$ layer [Fig. 1(b)], clear peaks owing to the polycrystallization were observed after annealing more than 300 °C. Similar results were obtained for undoped and P-doped samples as shown in Fig. 1(c), where we estimated the degree of crystallization [the percentage of the area intensities of peaks associated with the polycrystal phase shown in Figs. 1(a) and 1(b)] for all samples. Grazing angle X-ray diffraction (XRD) measurement for the B-doped $Si_{1-x}Sn_x$ layer [Fig. 2(a)] clarified that β-Sn precipitated in the layers after annealing more than 700 °C.

Next, we compared substitutional Sn contents in the poly-$Si_{1-x}Sn_x$ layers estimated from Raman and XRD analyses [Fig. 2(b)]. Although a comprehensive Raman study for $Si_{1-x}Sn_x$ has not yet been conducted experimentally, we can roughly estimate $x$ from recent molecular dynamics simulations reported by Ref. 6, where $\Delta\omega$ ($cm^{-1}$) $= -161.59x$ was obtained for the main peak of the Si–Si vibration mode in $Si_{1-x}Sn_x$. In our recent calculation based on density functional theory [7], the lattice constant of $Si_{8-n}Sn_n$ hardly deviated from Vegard's law; hence, we calculated the lattice constant from the peak position of the $Si_{1-x}Sn_x$ 111 and then corresponding substitutional Sn content was estimated from Vegard's law. Although the substitutional Sn contents estimated by Raman analyses show a high tendency compared with those estimated by XRD analyses for all samples, these Sn contents are almost consistent.

Finally, we present the thermoelectrical properties of the Si-rich poly-$Si_{1-x}Sn_x$ layers, measured at RT (Fig. 3). For undoped and B-doped $Si_{1-x}Sn_x$ layers, the electrical conductivity $\sigma$ (Seebeck coefficient $S$) increases (decreases) with the annealing temperature, suggesting an increase of the carrier density. For the P-doped $Si_{1-x}Sn_x$ layer, the opposite tendencies were obtained. As a result, a maximum power factor (PF=$S^2\sigma$) of 0.53 $\mu Wcm^{-1}K^{-2}$ was obtained for B-doped $Si_{1-x}Sn_x$ layers after annealing at 900 °C, although the PF for P-doped one is still low [Fig. 3(b)]. We propose that the dopant-dependent properties are related to whether dopant segregation during the growth occurs or not. This is because P atoms can easily segregate because of the small segregation coefficient in Si (0.35), which is smaller than that of B (0.80) [8]. Unfortunately, because of the low $\sigma$, the obtained PF is about 1/2 of that for Ge-rich poly-$Ge_{1-x}Sn_x$ on $SiO_2$ grown by SPC [9]. It is noted that the $\sigma$ in $Si_{1-x}Sn_x$ is at least one order lower than expected values from the Irvin curve of p- and n-type Si [10]; thus, the present study does not indicate the limitation of the potential of $Si_{1-x}Sn_x$.

## 4. Conclusions

Thermoelectric characterizations of undoped, B- and P-doped Si-rich poly-$Si_{1-x}Sn_x$ layers grown on $SiO_2$ were demonstrated. We found that although 900 °C-annealing caused significant Sn precipitation, the $\sigma$ for the B-doped samples showed a relatively high thermoelectric power (0.53 $\mu Wcm^{-1}K^{-2}$ at RT); in contrast, the that for P-doped one was still low due to decrease of $\sigma$ by the high-temperature annealing, which may cause the dopant segregation. We believe that continuing efforts open up the possibilities of high-quality $Si_{1-x}Sn_x$ essential for new group-IV thin-film TEGs.


## Acknowledgments

This work as partly supported by PRESTO (No. JPMJPR15R2) and CREST (No. JPMJCR19Q5) from the JST in Japan, and a research grant (Creation of life innovation materials for interdisciplinary and international researcher development) from the MEXT in Japan.



**References:** [1] S. N. Khatami *et al.*, Appl. Phys. Rev. **6**, 014015 (2016). [2] MK *et al.*, APL **106**, 171908 (2015). [3] MK *et al.*, APL **111**, 192106 (2017). [4] MK *et al.*, JJAP **58**, SAAD02 (2019). [5] H. Xia *et al.*, JAP **78**, 6705 (1995). [6] M. Tomita *et al.*, JJAP **57**, 04FB04 (2018). [7] Y. Nagae, MK *et al.*, JJAP **55**, 08PE04 (2016). [8] F. A. Trumbore, Bell Syst. Tech. J. **39**, 205 (1960). [9] MK *et al.*, ECS Trans. **75**, 481 (2016). [10] S. M. Sze and J. C. Irvin, Solid-State Electron. **11**, 599 (1968)


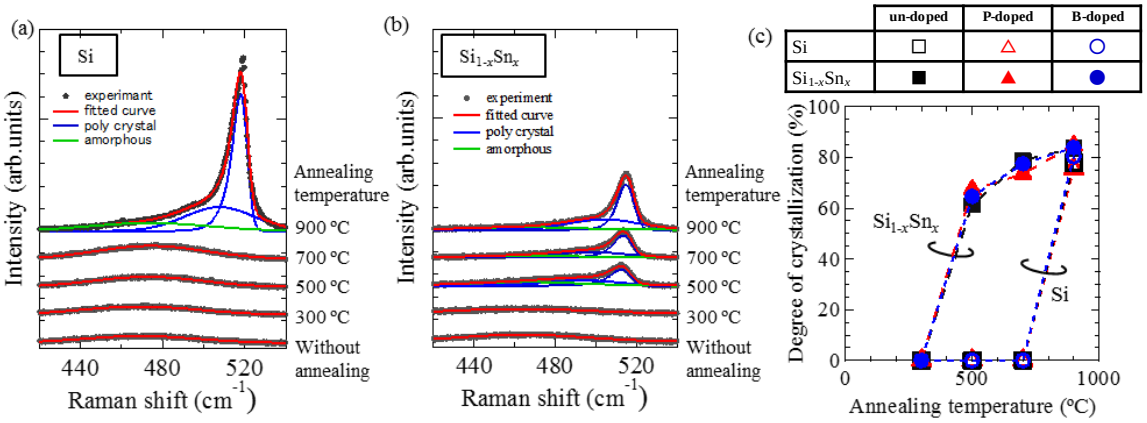


**Fig. 1** Raman spectra obtained from the (a) B-doped Si and (b) $Si_{1-x}Sn_x$ layers after annealing at 300-900 ºC samples before and after annealing at 300-900 ºC for 10 min. (c) Degree of crystallization of the Si and $Si_{1-x}Sn_x$ layers as a function of the annealing temperature. The initial content in the amorphous $Si_{1-x}Sn_x$ layers was 10 %.

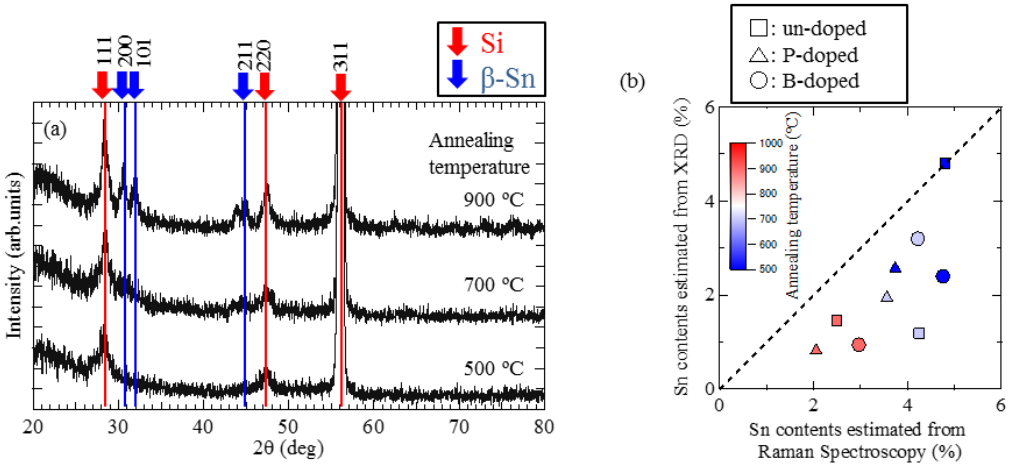


**Fig. 2** (a) Grazing angle XRD profiles obtained from the B-doped $Si_{1-x}Sn_x$ layers after annealing at 500-900 ºC for 10 min. (b) Comparison between the substitutional Sn contents in the various poly-$Si_{1-x}Sn_x$ layers estimated with Raman and that with XRD analyses. The color of marker corresponds to annealing temperature.

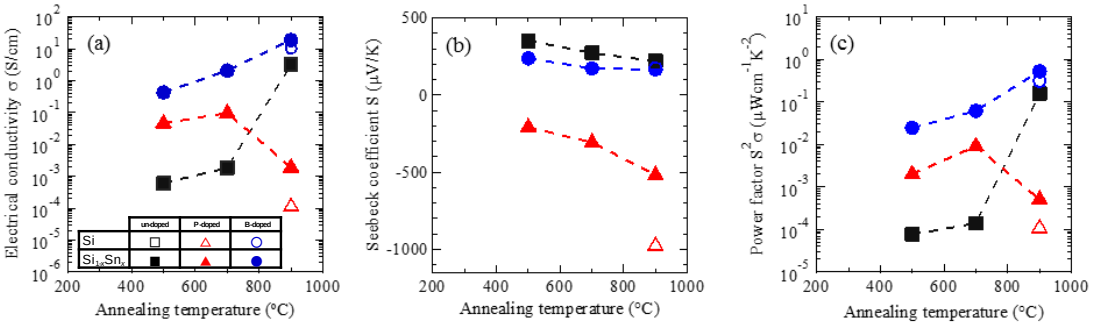


**Fig. 3** (a) Electrical conductivity, (b) Seebeck coefficient and (c) power factor of the un-doped, P- and B-doped Si and $Si_{1-x}Sn_x$ layers as a function of the annealing temperature.